Evaluation of spectral methods for high-frequency multiannual time series in coastal transitional waters: advantages of combined analyses: Tests of spectral analysis on coastal time series

Isabel Jalon Rojas, Sabine Schmidt, Aldo Sottolichio

LIMNOLOGY
and
OCEANOGRAPHY: METHODS

ASLO

Limnol. Oceanogr.: Methods 14, 2016, 381–396

doi: 10.1002/lom3.10097

Evaluation of spectral methods for high-frequency multiannual time series in coastal transitional waters: advantages of combined analyses

Isabel Jalón-Rojas,*[1] Sabine Schmidt,[2] Aldo Sottolichio[1]
[1]Univ. Bordeaux, EPOC, UMR5805, Pessac, France
[2]CNRS, EPOC, UMR5805, Pessac, France

Abstract

High-frequency monitoring is currently a major component in the management and research of the coastal system responses to ongoing global changes. This monitoring is essential in tidal systems to address the multiscale variability of physico-chemical parameters. The analysis of the resulting multiscale, nonlinear, non-stationary and noisy time series requires adequate techniques; however, to date, there are no standardized methods. Spectral methods might be useful tools to reveal the main variability time scales, and thus their associated forcings. The most widely used methods in coastal systems are Lomb-Scargle Periodogram (LSP), Singular Spectral Analysis (SSA), Continuous Wavelet Transform (CWT), and Empirical Mode Decomposition (EMD), but their relevance for high-frequency, long-term records is still largely unexplored. In this article, these spectral methods are tested and compared using a high-frequency 10-yr turbidity dataset in the Gironde estuary. Advantages and limitations of each method are evaluated on the basis of five criteria: (1) efficiency for incomplete time series, (2) appropriateness for time-varying analysis, (3) ability to recognize processes without complementary environmental variables, (4) capacity to calculate the relative importance of forcings, and (5) capacity to identify long-term trends. SSA is the only analysis method to satisfy all the criteria, even with 70% missing data. Combining methods is also a promising strategy; i.e., SSA + LSP for better recognition of processes; CWT + SSA and EMD + CWT for short-term (seasonal) and long-term (>1 yr) analysis, respectively. The purpose of this methodological framework is to serve as a reference for future post-processing of data from monitoring programs in coastal waters.

Coastal systems are highly dynamic and productive environments subject to permanent alteration and adaptation. They are often dominated by tides, which present a non-stationary and nonlinear behavior (Guo et al. 2015). Tidal propagation from open oceans and shelves to coasts and estuaries is modified by bottom friction, basin topography, and river discharge (Friedrichs and Aubrey 1988; Savenije et al. 2008; Sassi and Hoitink 2013). In the case of transitional waters, the system complexity is also promoted by the mixing between seawater and freshwater that results in rapid and strong physical, chemical and biological gradients. Human activities, for domestic, industrial, agricultural and touristic purposes, also induce variability in coastal environments (Kennish 2002), and, on longer timescales, meteorological and climatological variations can be significant (Scavia et al. 2002; Perillo and Piccolo 2011). The multiscale variability of tidal systems is thus hardly predictable, but is a key issue in environmental research and management.

*Correspondence: isabel.jalon-rojas@u-bordeaux.fr

In this context, time series of environmental variables from in situ measurements are essential to better understand aquatic systems and in particular to address water quality. Numerical models or remote sensing also require field data for calibration and validation at a relatively high sampling frequency. Over the last decade, monitoring programs of environmental parameters are increasingly widespread in coastal water systems (Dixon and Chiswell 1996; de Jonge et al. 2006; Goberville et al. 2010). They are promoted by directives and regulations, such as the European Union Water Framework Directive (WFD; Directive 2006/60/EC). The analysis of these time series has traditionally faced three difficulties: (1) inevitable gaps in data, limiting the post-processing, (2) the need for recording other environmental variables in the same period and at a coherent sampling frequency, and (3) the quantification of low-frequency variability that requires continuous measurements over long time periods. This latter problem can be solved through the recent development of high-frequency and long-term monitoring programs in coastal (Blain et al.

Table 1. Overview of the main published works using spectral methods in coastal environments. Works corresponding to high-frequency multiannual datasets are underlined, among which those recorded in estuaries are in bold.

Spectral method	Measured parameter and references
Power Spectrum Analysis (PSA)	Oxygen (Rabalais et al. 1994; **Schmitt et al.** 2008; Huang and Schmitt 2014; Rafelski et al. 2015)
	Phytoplackton (Platt 1978; Vasseur and Gaedke 2007; Derot et al. 2015)
	Salinity (Sikora and Kjerfve 1985; Reynolds-Fleming and Luettich 2004; Kbaier et al. in press)
	Temperature (Alvarez-Borrego and Alvarez-Borrego 1982; Dur et al. 2007; Kbaier et al., in press)
	Turbidity (Guézennec et al. 1999; Hoitink 2004; **Schmitt et al.** 2008)
	Water level (Luettich et al. 2002; Reynolds-Fleming and Luettich 2004; Kastens 2014)
	Waves (Pierson and Marks 1952;Sénéchal et al. 2002; Ruju et al. 2014)
Continuous Wavelet Transform (CWT)	Currents (Jay and Flinchem 1995; Uncles 2002; Matabos et al. 2014)
	Oxygen (Moore et al. 2009; Nezlin et al. 2009)
	Phytoplankton (Machu et al. 1999; Hodges and Rudnick 2006; Zhang et al. 2010a)
	Water level (Percival and Mofjeld 1997; Buschman et al. 2009; Zhang et al. 2010b; Guo et al. 2015)
	Waves (Meyers et al. 1993; Camayo and Campos 2006)
Singular Spectrum Analysis (SSA)	Beach shoreline (Różyński et al. 2001)
	Suspended sediment concentration (**Schoellhamer** 2002; French et al. 2008)
	Temperature (Keiner and Yan 1997)
	River flow (Knowles 2002)
Empirical Mode Decomposition (EMD)	Copepods (Schmitt et al. 2007)
	Oxygen (Moore et al. 2009; Huang and Schmitt 2014)
	Phytoplankton (Derot et al. 2015)
	River flow (Huang et al. 2009)
	Water level (Huang et al. 2000; Ezer et al. 2013)

2004; Pairaud et al. 2013; Rigby et al. 2014), estuarine (Etcheber et al. 2011; Contreras and Polo 2012; Jalón-Rojas et al. 2016) and lagoon systems (Andersen et al. 2006; Ciavatta et al. 2008). However, at present, there are no standardized methods to address such high-frequency multiannual datasets.

Time series analysis includes a large variety of techniques (Emery and Thomson 2001), ranging from the most classical statistical tools (e.g., descriptive statistics, probabilities, statistical tests, statistical distributions, regressions) to the relatively more recent spectral analysis. Spectral techniques are fundamental tools used by a multitude of disciplines (e.g., climatology, Ghil et al. (2002) to provide comprehensible and interpretable information in the frequency domain, which is especially efficient for identify underlying mechanisms (Fulcher et al. 2013). They are particularly relevant for multiscale non-stationary, nonlinear and noisy signals, such as those recorded in tidal systems (Puillat et al. 2014), by distinguishing between deterministic and stochastic processes. In coastal science, the four most commonly used spectral methods are Power Spectrum Analysis (PSA), Continuous Wavelet Transform (CWT), the Singular Spectrum Analysis (SSA) and Empirical Mode Decomposition (EMD) (Table 1). However, except for the classical PSA, they are still barely employed in the analysis of datasets from high-frequency multiannual monitoring, particularly in estuaries (Table 1). Therefore, a fundamental question is: which spectral methods are the most pertinent considering the particularities of these datasets?

This study presents a comparison of these four spectral techniques (Power Spectrum Analysis, Singular Spectrum Analysis, Wavelet Transform and Empirical Mode Decomposition) for the analysis of high-frequency multiannual time series recorded for coastal tidal systems. This test is performed using a high-frequency 10-yr turbidity record of the Gironde estuary (France). The main objective is to discuss the advantages and limitations of each method by considering the particularities and the analysis needs of such datasets, i.e., performance with missing values, identification of variability associated with factors other than tides, especially those of low frequency, quantification of the forcing influences, etc. The perspective of how the methods can complement each other is also discussed.

Methods

Turbidity time series in the Gironde estuary

The Gironde (SW France) is a macrotidal and hyper-turbid fluvial-estuarine system formed by the junction of the Garonne and Dordogne rivers. Its highly concentrated turbidity maximum, a region of high concentration of suspended sediments, forms by the trapping of fine sediment by the mechanism of tidal wave asymmetry within the estuary. The turbidity maximum shifts seasonally as a function

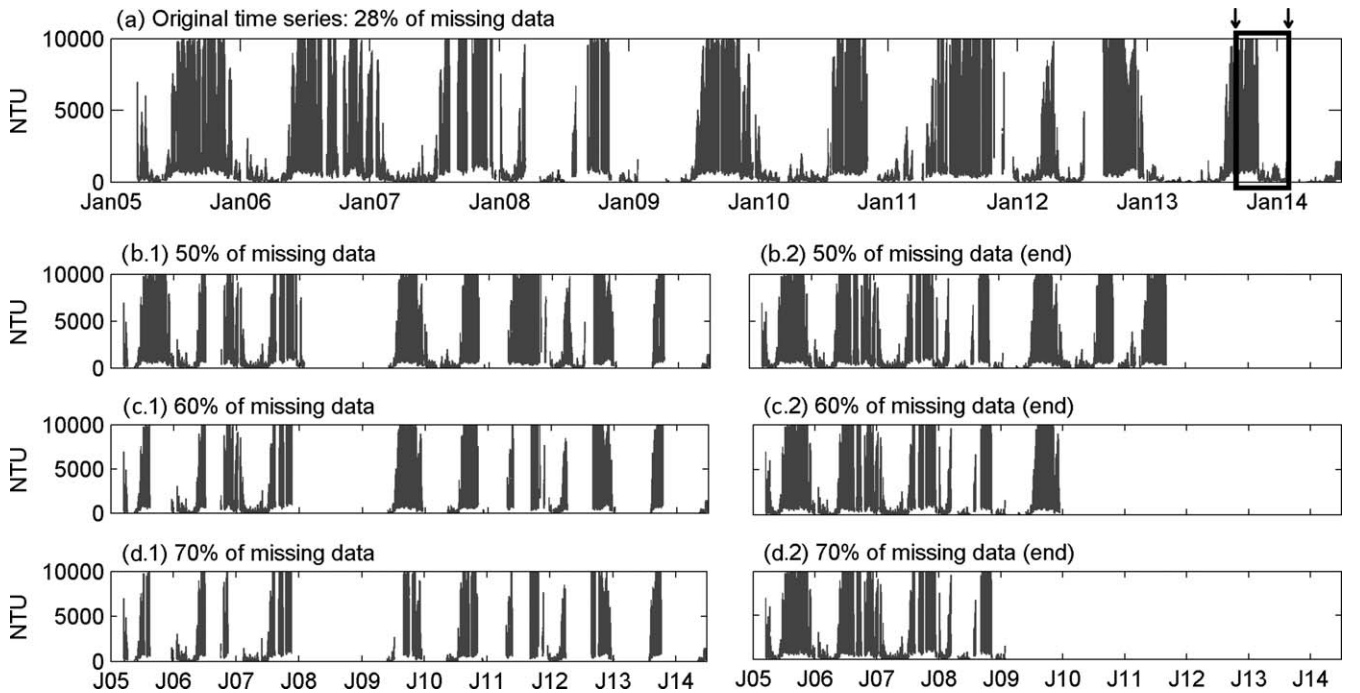

Fig. 1. (a) Time series of turbidity recorded at Bordeaux, the original dataset presents 28% of missing data. **(b–d)** Modified time series by: randomly deleting data from **(a)** to obtain 50% **(b.1)**, 60% **(c.1)** and 70% **(d.1)** of missing data; continuously deleting data at the end of **(a)** to obtain 50% **(b.2)**, 60% **(c.2)** and 70% **(d.2)** of missing data. The dark square shown by arrows in panel A refers to the data block analyzed by CWT (Fig. 3).

of river flow: it moves upstream during low river discharge periods (Castaing and Allen 1981; Jalón-Rojas et al. 2015) and is flushed downstream during high river flow periods. The Gironde estuary is one of the first estuarine systems in counting on an automated high-frequency long-term monitoring network of water quality, called MAGEST (MArel Gironde ESTuary). Since 2005, this network has measured dissolved oxygen, salinity, temperature and turbidity every 10 min at 1 m below the surface at four stations, including Bordeaux (Etcheber et al. 2011; Schmidt et al. in press).

Turbidity is a key parameter in estuaries: it is a surrogate for suspended sediment, which plays a fundamental role in sedimentary processes and water quality. Turbidity is a good example of a complex and hardly predictable variable. Various factors, such as physical forcings (turbulence, tidal harmonics, tidal range, river discharge, wind waves), engineering works and climatic changes, may cause its temporal and spatial variability at short and long time scales. After 10 yr, the Gironde's turbidity dataset includes contrasted hydrological situations and was recently analyzed in detail through descriptive and statistical tools (Jalón-Rojas et al. 2015), revealing the main trends in suspended sediment dynamics according to key forcings (fluvial discharge, tide).

To further this interpretation and determine the relative contributions of the different forcings, spectral analysis is required. Until now, few works have analyzed estuarine turbidity or SS time series through spectral analysis, such as PSA (Schmitt et al. 2008) and SSA (Schoellhamer 2002; French et al. 2008) (Table 1). There is no generic spectral method for such time series in transitional waters. The 10-yr turbidity time series at the Bordeaux station (from 2005 to 2014, Fig. 1a) is used as an example of a high-frequency multiannual dataset of a key parameter in coastal transitional waters. The four spectral methods are applied to this time series, which has a relatively high rate of proper operation, presenting only 28% missing data. Data corresponding to the saturation value of the turbidity sensor (9999 NTU; Jalón-Rojas et al. 2015) account for only 2% of the time series and occur during periods shorter than 2 h. We analyze the available data rather than fill gaps, which would imply knowledge of the trends.

Spectral methods

Power spectrum: Lomb-Scargle periodogram (LSP)

The power spectrum or periodogram is the classical analysis of time series decomposition into periodicities, which are defined as sinusoids. It shows the energy of these periodicities as a function of frequency. Traditional mathematical methods, such as classical periodograms obtained from Fast Fourier Transform (FFT, Blackman and Tukey 1958; Welch 1969), require equidistant time series without any gaps. However, periodogram of non-equidistant time series can be now calculated using methods such as the FFT of

autocorrelation functions (Wiener-Khinchin theorem, see Gardiner 1985), the Lomb-Scargle periodogram (Lomb 1976; Scargle 1982; Press et al. 1992) or Hilbert Spectral Analysis (Huang et al. 1998, 1999).

Based on the least squares method, the Lomb-Scargle periodogram (LSP), named for Lomb (1976) and Scargle (1982), is currently a classic method for finding periodicity in irregularly sampled data. It is equivalent to fitting sine waves of the form $y = a\cos\omega t + b\sin\omega t$. An extensive discussion of the method was given in Van Dongen et al. (1997). We used the *lombscargle* algorithm in Press et al. (1992) implemented in MATLAB by Brett Shoelson, which also provides significance levels. The efficiency of this algorithm for incomplete time series has been widely recognized in several disciplines (Ruf 1999). Quite recently, Kbaier et al. (in press) has tested its capability to detect significant frequencies using a 1-yr high-frequency time series of salinity in the eastern English Channel with 18.76% missing data. This work suggests that seasonal variability is not accurately detected beyond 50% missing data for short time-series (<1 yr). The limit of this method in multiannual time series is still unknown.

Continuous wavelet transform (CWT)

Wavelet analysis decomposes a time series into time frequency space. A wavelet spectrum (or scalogram) represents the energy variations along time and frequency, providing the dominant variability modes and how those modes vary over time. The approach selected here is the continuous wavelet transform (CWT). While the discrete wavelet transform is preferred for data compression, the CWT is generally better for dynamical analysis (Farge 1992), and is thus the usual approach employed in coastal research (Table 1). The CWT is based on a wavelet function that acts as a band-pass filter to the time series. The choice of the wavelet function is crucial for adequate results. We use the Morlet function which is nonorthogonal, complex and seems to offer a good trade-off between detecting oscillation and peaks or discontinuities (Setz 2011). The effectiveness of this function has been widely recognized for tidal signals because it satisfies the admissibility condition (i.e., the wavelet oscillates with its mean value equal to zero) (Daubechies 1992; Farge 1992; Guo et al. 2015). One may refer to Torrence and Compo (1998) for a general overview of Morlets wavelets and their application in geophysical and oceanographic studies. The main drawback of wavelet analysis is the need of equally sampled data. Recent efforts in adapting wavelets to incomplete time series by interpolating periods across missing data (e.g., Harang et al. 2012) have been able to solve small gaps in the sinusoidal signal. However, to our knowledge, there are still any algorithms appropriate for complex long-term time series presenting long gaps. Here, we use the MATLAB wavelet coherence package developed by Grinsted et al. (2004).

Singular spectral analysis (SSA)

Singular spectrum analysis (SSA) is essentially a principal component analysis in the time domain (Vautard et al. 1992; Schoellhamer 1996). It has been demonstrated to be especially efficient for extracting information from short and noisy time series without previous knowledge of the (nonlinear) dynamics affecting the time series (Vautard et al. 1992; Dettinger et al. 1995; Schoellhamer 2002). SSA is based on the idea of sliding a window of width M down a time series to obtain an autocorrelation matrix (Vautard et al. 1992). Eigenvectors (empirical orthogonal functions) and eigenvalues, λ, of the lagged autocorrelation matrix are then calculated. The time series is decomposed into simpler time series, the so-called reconstructed components (RCs), by multiplying eigenvectors and their corresponding principal components (calculated by multiplying eigenvectors and data). Each RC is nearly periodic with one or two dominant periods. The contribution of the variance of each period is given by its corresponding λ. Most of the variance is contained in the first RCs, and the remaining RCs contain noise. The representation of λ in order of decreasing magnitude exhibits a steep initial slope containing the significant components, which is followed by a flatter floor that represents the noise level (Vautard et al. 1992). For further information about the method, the reader is referred to Vautard et al. (1992) and Ghil et al. (2002).

There are two options to analyze datasets containing missing data through SSA. First, Schoellhamer (2001) developed a modified singular-spectrum analysis (SSAM) algorithm to obtain RCs from records with a large fraction of missing data. The alternative consists of estimating the RCs in gaps through temporal correlations provided by the gap-filling version of SSA (Kondrashov and Ghil 2006; Kondrashov et al. 2010). Because we do not fill data gaps, this implies using Schoellhamer's SSA algorithm. The lagged autocorrelation is computed by ignoring any pair of data points with a missing value. When computing each value in a principal component series, if the fraction of missing data is within the window $M \times f$, then that value is assigned a missing value (Schoellhamer 2001, 2002). No method or algorithm was specified to calculate the period of the modes including missing data. Schoellhamer (2001) tested the ability of SSAM to process missing data using a 1-yr synthetic high-frequency time series that followed the characteristics of suspended-sediment concentration from San Francisco Bay. This test demonstrated this method to be efficient with 50% missing data. Here, we test the SSAM limits for incomplete multiannual continuous time series using the Schoellhamer's algorithm available for MATLAB with $f = 0.5$.

Empirical mode decomposition (EMD)

The empirical mode decomposition (EMD) is a relatively recent method for time-frequency data analysis developed by Huang et al. (1998). It decomposes a signal into a finite and

often small number of simpler time series or modes, the so-called intrinsic mode functions (IMFs), and a residual. The EMD works as an algorithm that, in each iterative step, considers the signal as a sum of a low frequency part (residual) and a high frequency part (IMF). The procedure is repeated for the residual, considered as a new times series, extracting a new IMF using a spline function, and obtaining a new residual until no more IMF can be extracted (Huang et al. 1998; Rilling et al. 2003; Huang and Schmitt 2014). Each IMF is an oscillation time series with a zero mean and a characteristic frequency. The final result is thus a frequency-time distribution of unit-energy signal. This method is particularly suitable for non-linear and non-stationary processes because it is based on the local characteristics of the data time scale (Huang et al. 1999; Flandrin et al. 2004). It can be applied to time series with irregular time intervals (Huang et al. 1998; Flandrin and Gonçalvès 2004) because the information is contained at the local extrema. For a detailed description, the reader is referred to Huang et al. (1998) and Flandrin et al. (2004). Here, we use the MATLAB algorithm implemented by Rilling et al. (2003). The mean period ($\bar{T}$) of each IMF mode (n) is estimated by calculating the local extrema and zero-crossing points (Rilling et al. 2003; Huang et al. 2009; Huang and Schmitt 2014), i.e.,

$$\bar{T} = \frac{L}{N_{n,\max} + N_{n,\min} + N_{n,0}} \times 4 \quad (1)$$

in which L is the length of the data.

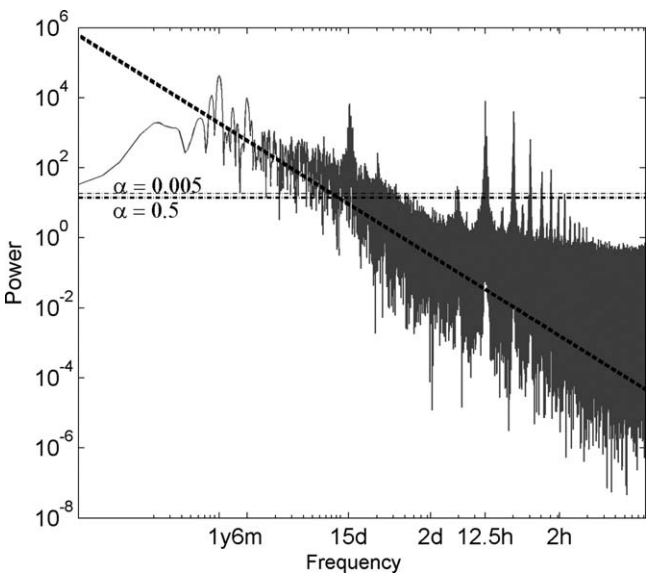

Fig. 2. Lomb-Scargle periodogram of the original turbidity time series at Bordeaux (Fig. 1a). Horizontal dotted grey lines represent the significance levels (α) of 0.005 and 0.5. Dark dotted line corresponds to the power law of turbulence: $E(f) \approx f^{-5/3}$.

Evaluation criteria

The criteria to evaluate advantages and limitations of each spectral method were chosen first by considering the traditional difficulties in the time series analysis of water systems (i.e., presence of gaps, limitations for short term analysis and the need of complementary environmental variables). Second, we tested the capacity to extract additional information, such as the relative importance of processes or forcings, which are difficult to obtain with classical descriptive or statistical tools. The five criteria used in this work are thus: (1) efficiency for incomplete time series; (2) appropriateness for time-varying analysis; (3) ability to recognize processes without the necessity of complementary environmental variables; (4) capacity to calculate the relative importance of forcings; (5) capacity to identify long-term trends.

Table 2. Significant time scales recognized by the LSP applied to time series presenting different percentages of missing data, suppressed randomly or continuously (Fig. 1).

	Missing data (%)						
		Randomly			Continuously		
Significant time scales	28	50	60	70	50	60	70
~1 yr	x	x	x	X	x	x	x
~6 months	x	x	x	X	x		
14.8 d	x	x	x	X	x	x	x
7.4 d	x	x	x	X	x	x	x
1 d	x	x	x	X			
12.48 h	x	x	x	X	x	x	x
6.21 h	x	x	x	X	x	x	x
4.09 h	x	x	x	X	x	x	x
3.12 h	x	x	x	X	x	x	x
2.4 h	x	x	x	X	x	x	x

To assess the efficiency for incomplete time series of each method (except CWT), we progressively deleted data from the original turbidity time series (28% missing data, Fig. 1a) to obtain time series with missing data rates of 50%, 60%, and 70%. We suppressed data in two different ways: (1) randomly to reproduce the typical gaps in the monitored time series (Fig. 1a, b.1 and c.1); (2) continuously at the end of the time series to compare the influence of the measurement duration (Fig. 1a, b.2 and c.2). We then applied each of the four spectral methods to the original and the six modified time series and compared the main outputs considering:

- the number of significant frequencies detected for the LSP;
- the characteristic frequency of each RC and its percentage of contribution to the variance for the SSA;
- the characteristic frequency of each IMF for the EMD;

Results and discussion

Lomb-Scargle periodogram (LSP) test

Figure 2 illustrates the LSP of the original turbidity time series in a log-log plot. It shows the main variability time scales, i.e., those associated with energy values above significance levels (α) of: (a) 366 d, (b) 183 d, (c) 14.8 d, (d) 7 d, (e) 1 d, (f) 12.48 h, (g) 6.24 h, (h) 4.09 h, (i) 3.12 h, and (j) 2.4 h. These time scales are easily linked to deterministic forcings: seasonal river flow changes (a,b), tidal harmonics (d–i) and tidal range (c,d). The method allows for sorting variability time scales and their associated forcing by increasing order of importance: 1 yr (river flow), 6 months (river flow), 12.48 h (semidiurnal tide), 14.8 d (tidal range) and 6.12 h (quarterdiurnal tide). However, the impossibility of a time-varying analysis does not permit assessment of the variability of the relative contributions of forcings with time. In addition, the method is not able to document multiannual variability due to the lack of significant variability at time scales greater than 1 yr. Alternatively, the power law behavior ($E(f) \approx f^{-\beta}$) of the spectrum trend gives scaling properties of variables (Schmitt et al. 2008; Zongo and Schmitt 2011; Derot et al. 2015). The scaling exponent β is equal to 0 for noise, 2 for Brownian motion and 5/3 for turbulence (Huang et al. 2008). For turbidity in the Gironde estuary, the LSP reveals a turbulent-like behavior of turbidity on time scales between 10 min and 1 yr (dark dotted line in Fig. 2).

There is a difference in the two series of tests of incomplete time series (Table 2). The LSP method recognizes all the significant time scales in time series with randomly suppressed data, even with 70% missing data. When the time series is shortened by deleting a block of continuous data, the method is less efficient in detecting significant time scales. In particular, it does not detect the 1-d time scale, which is just above the significance levels. The 6-month time scale is also not detected for incomplete time series with 60% and 70% missing data suppressed continuously. This is consistent with the conclusion of Kbaier et al. (in press)

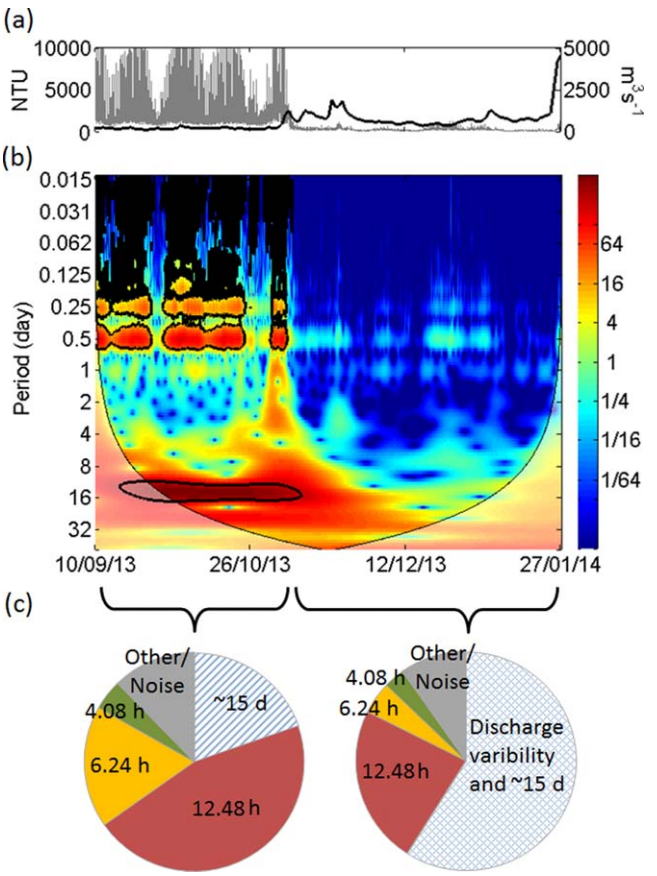

Fig. 3. (a) Garonne river flow (black) and continuous turbidity data (grey) of 4.5 months (from September 10th 2013 to January 27th 2014). **(b)** Corresponding continuous wavelet spectrum of turbidity normalized by the variance (color bar). The thick black contour designates the 5% significance level against red noise. The cone of influence (COI), where edge effects might distort the picture, is shown as a lighter shade. **(c)** Contribution (%) of the different time scales to the turbidity variability (λ) calculated from SSA for periods of low and high river discharge. Note that SSA does not differentiate the contribution river flow and spring/neap tidal cycles for 3-month time series.

based on a 1-yr salinity time series, suggesting that the seasonal variability is susceptible to be undetected by the LSP applied to shorter time series with missing data. The present LSP test demonstrates its efficiency for multiannual incomplete series (Table 2). We also show that it is preferable to have a time series of at least 10–15 yr when 50% of the data are missing.

Continuous wavelet transform (CWT) test

The continuous wavelet was applied to a block of 140 d (dark square, Fig. 1a) of nearly continuous data (Fig. 3a,b). This dataset contains negligible gaps representing 0.6% of missing values; therefore, interpolation does not introduce significant errors. CWT analysis shows the temporal variability of the energy (bar color) of the time scales ranging from over 22.5 min to 50 d, i.e., the maximum identified time scales represented 35.7% of the block duration. The most

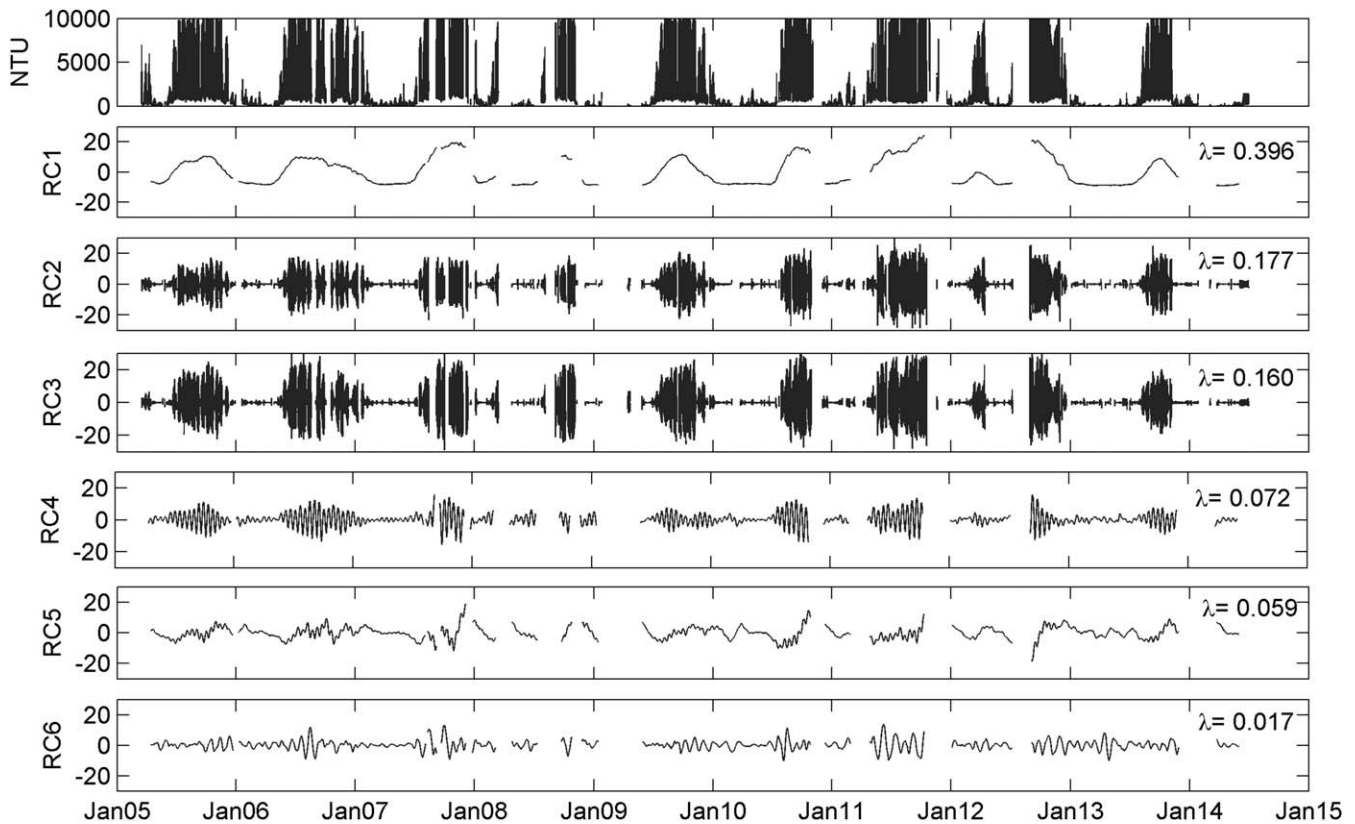

Fig. 4. Singular spectrum analysis (SSA) results for the turbidity time series (NTU) at Bordeaux (January 2005–July 2014). Factors associated to each RC are: drastic changes in discharge (RC1), semidiurnal tides (RC2), tidal frequencies below the semidiurnal (RC3), semimonthly tidal cycles (RC4), discharge variability (RC5), and monthly tidal cycles (RC6). λ is the contribution of each RC to the total turbidity variance, these 6 modes contain 88.1% of the variance.

obvious result is the presence of two marked periods. Between September 10th and November 8th, time scales associated with tidal cycles are clearly predominant: 14.8 d (half synodic month controlling tidal range), 12.5 h (semidiurnal tide), 6.2 h (quarterdiurnal tide) and other tidal harmonic frequencies. From November 8th, these tide-related energies are still observed, but eclipsed by the energetic time scales higher to 14.8 d. The factor responsible for this drastic change is the increase in river flow (Fig. 3a). This demonstrates that the main forcings have been recognized without prior knowledge of estuarine turbidity dynamics. Even if the effect of river flow seems the most important, the absence of its variability time scale in the scalogram makes a comparison difficult. The limitation due to missing data hampers long-term analysis. Nonetheless, the CWT method is very visual in the time domain, permitting to the differentiation between periods dominated by deterministic or stochastic processes.

Singular spectrum analysis (SSA) test

The first step in the application of SSA is the choice of the window size M. Typically, SSA successfully identifies periods in the range of 0.2 M–M. One or two RCs contain variations in the time series with periodicities greater than M (Schoellhamer 2002). Following this principle, SSA was first applied to raw turbidity with a window size M of 150 (i.e., 25 h since turbidity is collected every 10 min) to identify small variability time scales. To identify large scales, SSA was then applied to the tidally averaged turbidity time series with a windows size M of 100 (i.e., 1250 h, time step of 12.5 h). Tidal averages were calculated by averaging turbidity between the time intervals corresponding to the zero up-crossing values of tides. To calculate the relative contribution of a given RC from the 12.5 h-pass time series, its eigenvalue was multiplied by the ratio of the variance of the time series used for that pass to the variance of the original time series. For more information about the combined use of different time steps in SSA, the reader is referred to Schoellhamer (2002). Figure 4 presents the final result of the turbidity time series decomposition in six RCs, showing their respective contribution to the variance (λ). These RCs represent 88.1% of the total variability.

In the absence of a reference procedure to calculate the characteristic time scales of RCs presenting gaps, here we propose a methodology. As previously highlighted, LSP is efficient for detecting the main time scales of time series with missing data. Figure 5 shows the LSP of the RC2 and RC5, which provides their variability time scale.

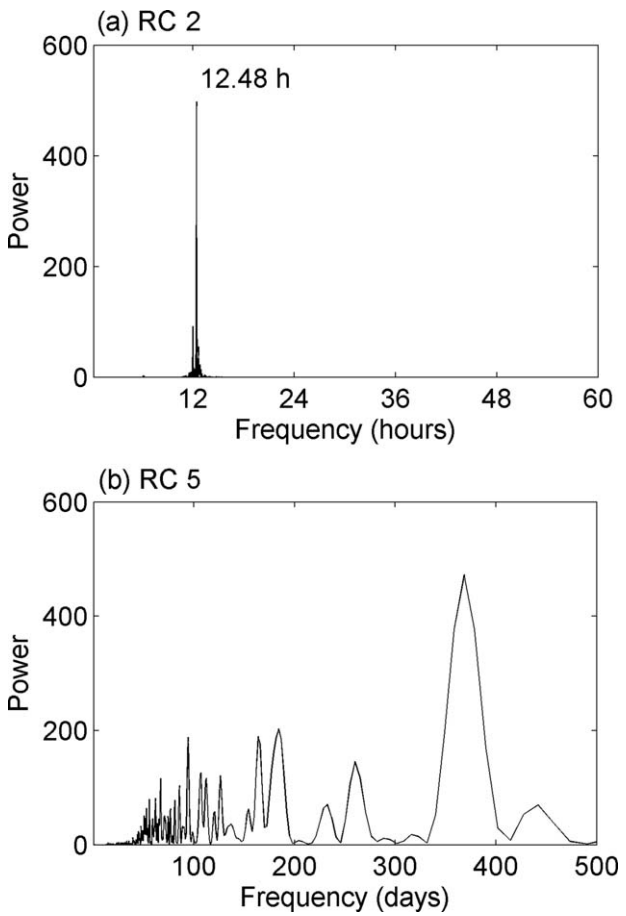

Fig. 5. Lomb-Scargle periodograms of the RC 2 **(a)** and RC 5 **(b)** resulting of applying SSA to the turbidity time series (see Fig. 4).

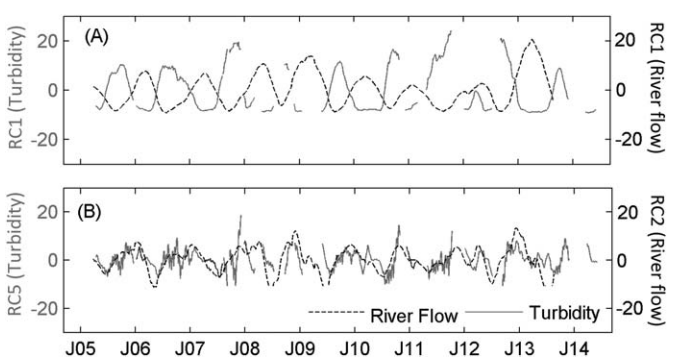

Fig. 6. Comparison of the RC 1 **(a)** and RC 5 **(b)** turbidity modes (Fig. 4) with the first and second modes from the decomposition of the time series of river flow through SSA, respectively.

Therefore, here we propose the use of the LSP. However, as it can require a high computational cost, we also propose the mode of periods between zero-crossing points, but only for RCs whose graphical representations exhibit an evident constant period (the average may be biased by gaps).

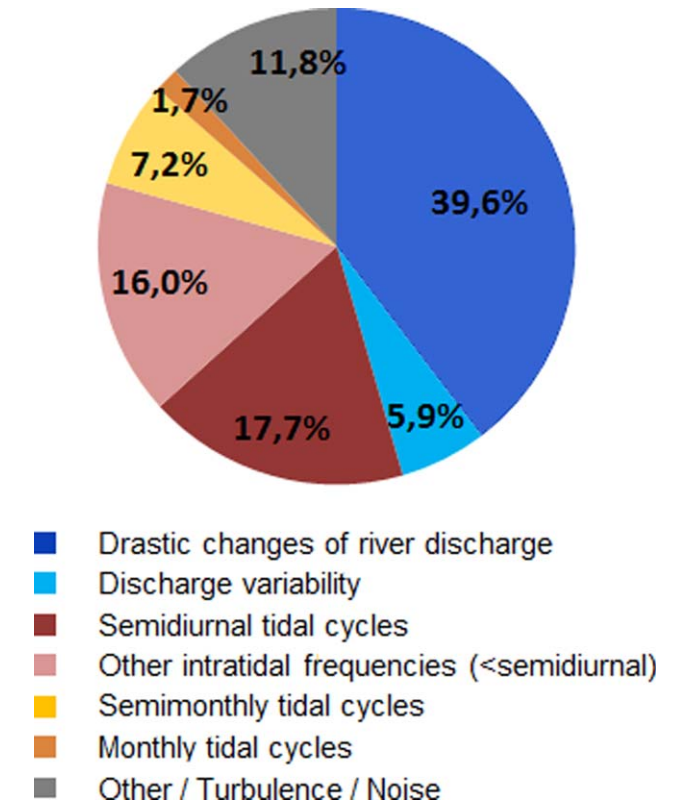

Fig. 7. Contribution of each factor to turbidity variability resulting of applying SSA.

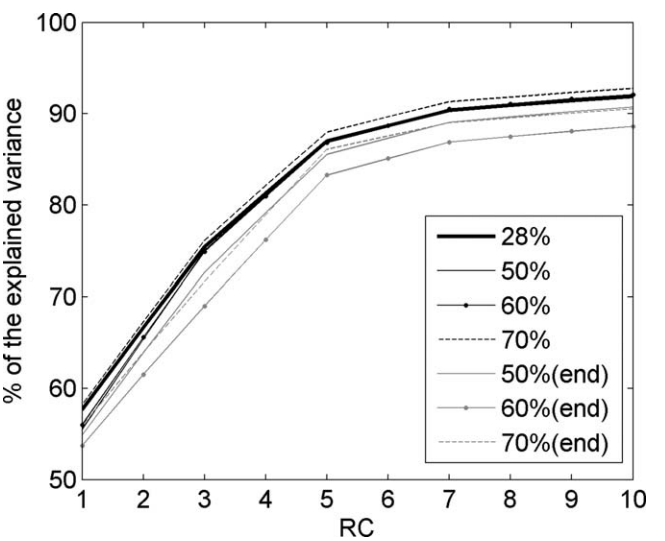

Fig. 8. Comparison of the cumulative turbidity variance (λ; %) of the ten first modes (RCs) calculated from turbidity time series presenting different percentages of missing data (Fig. 1).

Time scales were assigned to RCs following the above methodology: (RC1) ~1 yr and ~6 months; (RC2) 12.48 h; (RC3) sum of RCs with time scales of 6.24 h, 4.09 h, 3.12 h,

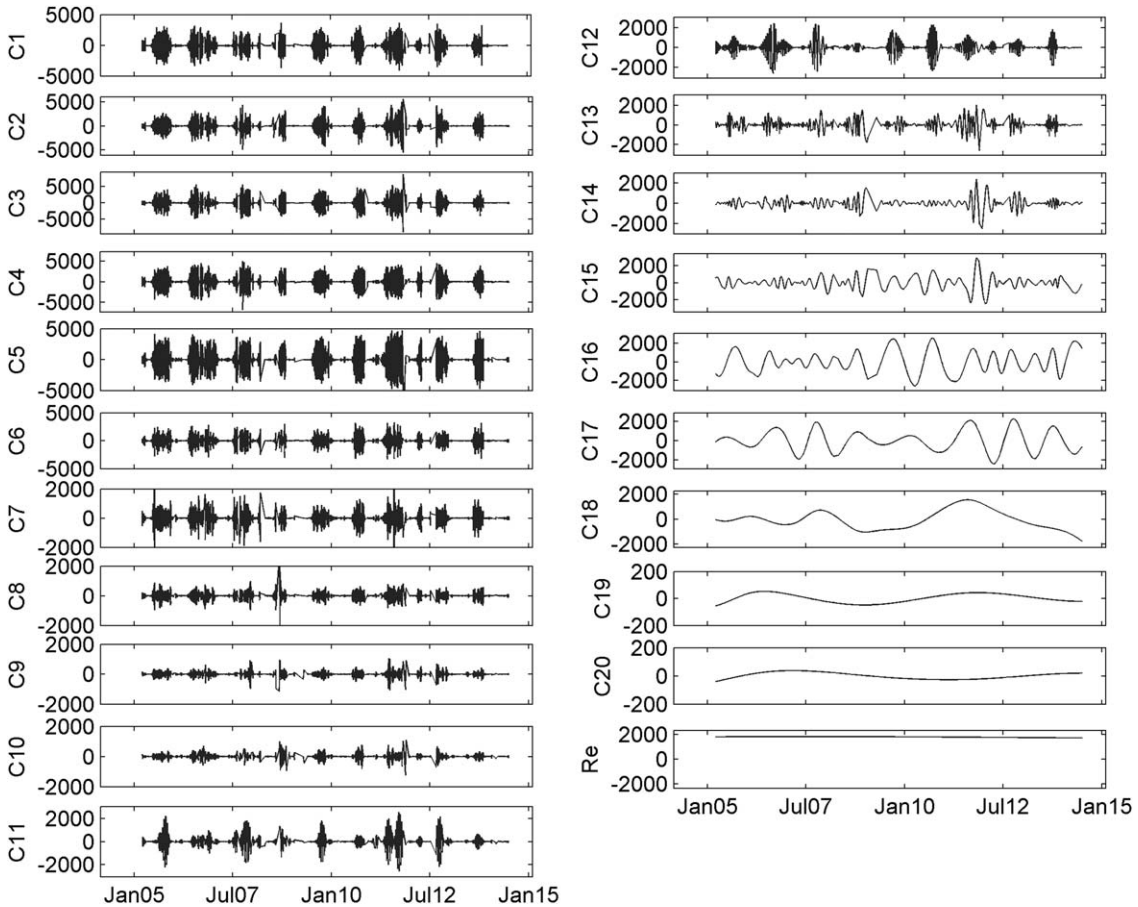

Fig. 9. IMF components of the turbidity time series at Bordeaux from EMD method: the mean time scales increase with the order of the modes.

2.4 h; (RC4) 14.8 d; (RC5) irregular time scale; (RC6) 30 d. Except for RC5, RCs and their contributions to the variance were easily attributable to specific forcings, without prior knowledge: river flow changes (RC1, 39.6%), semidiurnal tides (RC2, 17.7%), tidal frequencies below the semidiurnal frequency (RC3, 16%), semimonthly tidal cycles (RC4, 7.2%), and monthly tidal cycles (RC6, 1.7%). RC5 presents multiscale behavior (Fig. 5b) and, to be related to a forcing, the comparison to other environmental variables is required.

The high sensitivity of turbidity to river discharge in Bordeaux, located in the upper reaches of the Gironde estuary, suggests a relationship between this forcing and the RC5 mode. This hypothesis was tested by applying SSA to the Garonne river flow time series. RC1 modes of turbidity and discharge display opposite trends (Fig. 6a), confirming that the drastic changes of river flow act as a forcing. River flow RC2 and turbidity RC5 follow the same trend (Fig. 6b), indicating that the river flow variability explains RC5. Such trends and relationships are useful for characterizing long-term trends; even multiannual variability can be distinguished.

The final result of forcings affecting turbidity and their relative importance is summarized in Fig. 7. SSA allows to compare the contribution of tide and river flow on turbidity variability but also to differentiate the rather stochastic (river flow variability) and more deterministic (seasonal river flow changes) contributions of the same forcing. These quantifiable and easily interpretable results aim to be powerful tools to compare the contribution of forcings during hydrologically contrasted years, in different estuarine regions or even in different estuaries.

We applied SSA to the time series with different percentages of missing data to test its effectiveness (M of 150, time step of 10 min). For each considered turbidity dataset, each mode presents the same time scales as the original dataset. All the forcings were recognized, even with 70% missing data. The cumulative percentages of variability explained by the first modes of each time series are compared in Fig. 8. Modes from time series with randomly deleted missing data (black lines) explain almost the same percentages of variance as the original time series. Modes of shorter time series (grey lines) show slightly lower percentages, but the cumulative contribution to the variance is less than 5% lower than the original dataset.

Empirical mode decomposition (EMD) test

The turbidity time series of Bordeaux was decomposed through the EMD into 20 IMF modes plus the last residual

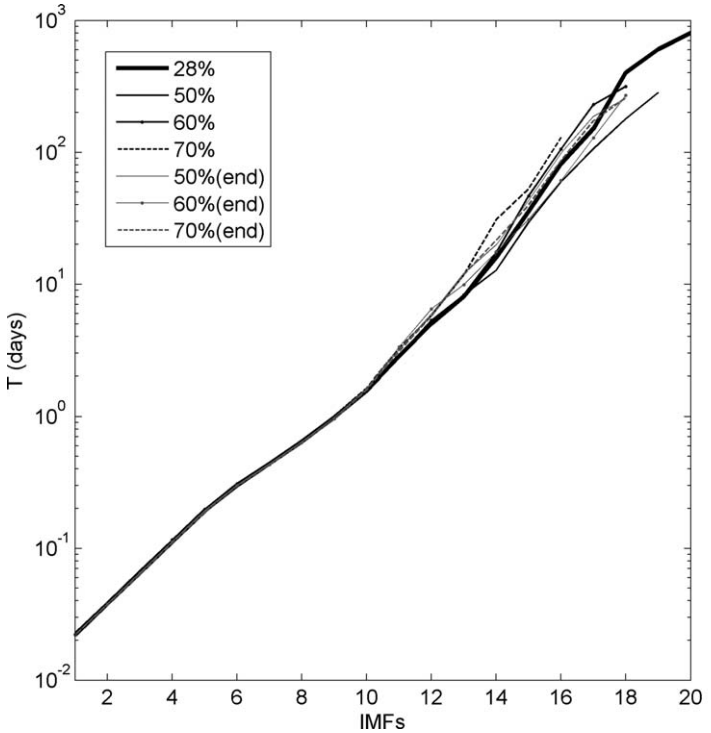

n	$\bar{T}$	LSP periods
1	0.53 h	
2	0.91 h	
3	1.57 h	
4	2.69 h	2.4 h
5	6.61 h	4.09 h
6	7.22 h	6.24 h
7	10.52 h	12.48 h
8	15.48 h	12.48 h
9	23.60 h	24 h
10	2 d	
11	3 d	
12	5 d	
13	8 d	7 d
14	16 d	15 d
15	36 d	
16	82 d	
17	151 d	182 d
18	403 d	365 d
19	604 d	
20	806 d	

Fig. 10. Mean time scales ($\bar{T}$, Eq. 1) of IMF modes obtained from EMD applied to turbidity time series presenting different percentages of missing data (Fig. 1). Table specifies $\bar{T}$ of each mode of the original turbidity time series (28% of missing data) and the mean time scales calculated from LSP (Fig. 2).

(Fig. 9). Each mode indicates the variation of a time scale. The mean time scale of the 20 modes is shown in Fig. 10. The time scales ($\bar{T}$) increase with the number of IMF modes (n), whereby the method does not directly provide the main variability time scales, which can be related to the main processes. Surprisingly, time scales were not precisely detected if they are compared with those of LSP (see Table in Fig. 10). For example, we can use IMF 7 or IMF 8 to explore turbidity variability at a time scale close to the semidiurnal tidal scale, but we cannot associate the turbidity variability to the different tidal harmonics and determine which is the most important intertidal variability time scale. Therefore, the analysis of deterministic forcing is imprecise and requires prior knowledge of the dynamics or needs to be complemented by other analyses, such as a power spectrum. Even to identify modes related to stochastic processes, they must be compared with the environmental variable representing the forcing or with the equivalent IMF mode of such environmental variables (e.g., the relationship between temperature and oxygen is given in Huang and Schmitt 2014).

After decomposition, the original time series can be separated into two terms: small (<1 month) and large scale fluctuations calculated as the sum of the high (from 1 to 14) and low (from 15 to 20 and the residual) frequency modes, respectively. The large-scale term gives the seasonal and interannual variability of turbidity as shown by its representation superposed to the original time series (Fig. 11a). The EMD method acts appropriately as a low-pass filter that accurately captures the multiscale long-term behavior of parameters. However, if the time series presents long gaps the large-scale term could be biased. In addition, the analysis of the multiannual variability could be analyzed through IMFs 18-20.

Time scales of modes resulting from the test on incomplete time series are compared in Fig. 10. Small-scale modes (<8 d) present quite similar time scales. In contrast, the number and characteristic frequency of large-scales modes vary between time series. This shows the randomness of the method in terms of detecting time scales and the main forcing affecting the variable. Nevertheless, note that the reconstructions of the long-term signal correctly follow the trend of its respective incomplete time series.

Added value of combined approaches

Spectral techniques are usually applied independently in coastal research (Kastens 2014). In studies based on high-frequency long-term series, only PSA and EMD were used in the same work (Huang and Schmitt 2014; Derot et al. 2015); the interest of this combination was illustrated in the previous section. Even if the spectral methods share the same finality of providing the main time scales of variability in time series, the present evaluation shows that they reveal different and, often complementary, aspects of the involved physical processes. The different tests based on the 10-yr

turbidity time series allowed us to discuss the advantages of combining methods and propose the best combinations.

As previously discussed, LSP is a useful method for calculating the time scales of RCs from SSA. It can also support the selection of the most pertinent number of modes. SSA gives a high number of modes (RCs), but the first ones contain most of the time series variability. The last significant RC according to the representation of the fractions of the variance λ in decreasing order of magnitude (see "Methods") was 2.4 h (one of the component of RC3, Fig. 4). This time scale also corresponds to the lowest significant tidal harmonic frequency provided by LSP (Fig. 2). In addition, LSP provided the contribution of turbulence in turbidity variability (Fig. 2), which to a large degree, may explain the unexplained variance (11.8%) resulting from SSA.

The main interest of CWT is the visual comparison of the relative importance of time scales, and their associated forcings, over time. As illustrated in Fig. 3, CWT readily differentiates two periods that present different trends in time scale importance (Fig. 3B). The application of SSA to each period separately permitted the calculation of the associated changes in the contributions of the different forcings (Fig. 3c). SSA complements CWT in terms of quantification, and CWT complements SSA by offering a more visual time-varying representation and helping the determination of interesting periods of application. Given the ineffectiveness of CWT for incomplete time series, the CWT–SSA combination is only possible for short-term analyses, considering the frequency and duration of gaps in environmental time-series.

We propose a solution to circumvent this problem of missing data for long-term CWT analyses. The sum of low frequency EMD modes gives a realistic multiscale long-term signal of variability (Fig. 11a). This signal can be interpolated to a regularly spaced time series that mimics the original and can be analyzed by CWT. The application of CWT offers the time-varying importance of long time scales (Fig. 11b): seasonal, annual and even multiannual (2007, 2010, 2011, and 2012 presented higher variability). For long-term analysis, EMD lets CWT decompose the larger variability time scales and CWT gives more visual and comprehensible information than the simple long-term signal from EMD.

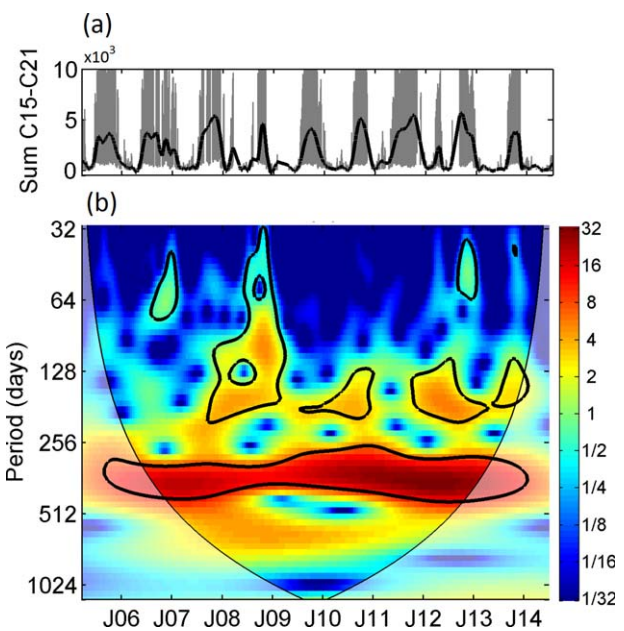

Fig. 11. **(a)** Turbidity time series at Bordeaux (grey) and reconstruction from IMF components (sum of C15–C21, black). **(b)** Wavelet spectrum of the IMF components reconstruction normalized by the variance (color bar). The thick black contour designates the 5% significance level against red noise. The cone of influence (COI), where edge effects might distort the picture, is shown as a lighter shade.

Synthesis and conclusions

The relevance of spectral analysis (Lomb-Scargle Periodogram, Singular Spectrum Analysis, Continuous Wavelet Transform and Empirical Mode Decomposition) has been evaluated for multiscale, nonlinear, non-stationary and noisy time series from in situ high-frequency multiannual coastal monitoring. We used the 10-yr turbidity time series recorded in the fluvial Gironde estuary at the time step of 10 min

Table 3. Pertinence of each tested spectral analysis and of combined methods regarding the five selected criteria. Symbols represent the efficiency of methods from low (−) to particularly good (++). (0) the method does not admit the evaluation of the criterion.

	Efficiency gaps	Time-varying analysis	Recognizing process	Relative importance of forcings	Long-term analysis
PSA (LS)	+	−	+−	+−	−
CWT	0	++	+−	+−	−
SSA	+	+	+	+	+
EMD	+−	+	−	−	+
SSA + LS	+	+	++	+	+
CWT + SSA	0	++	++	++	−
EMD + CWT	+−	+	− (+for long-term)	− (+for long-term)	++

since 2005. This parameter presents a mixed signal consisting of harmonic and stochastic components, equivalent to those observed for most physical-chemical parameters in coastal transitional waters. The advantages and limitations of each method were tested using five criteria: efficiency for incomplete time series, appropriateness for time-varying analysis, ability to recognize processes without the necessity of complementary environmental variables, capacity to calculate the relative importance of forcings, capacity to identify long-term trends (Table 3).

Briefly, the reliance of each is summarized below and in Table 3:

- LSP is particularly effective for recognizing periodical forcing, even with 70% missing data, but less suitable for evaluating non-periodic long-term trends. It is more effective with longer (7–10 yr) time series. The impossibility of a time-varying analysis downplays its high capacity to identify and rank the main processes.
- CWT is able to determine the dominant processes and how their contributions vary over time. It shows lower frequency resolution than LSP or SSA, but a more visual representation over time. Its limitations in terms of regularly sampled data restrict its use to complete time series, hampering the identification of all the processes and long-term analyses.
- SSA is the only analysis to reach all the criteria. It is very powerful for identifying deterministic processes but also stochastic processes, even if this requires minimal knowledge of the system or comparison with other environmental variables. SSA quantification of the contribution to the variance (in %) of modes is a great advantage over the other methods in term of comparing the importance of forcings. SSA also allows a long-term analysis.
- EMD is the least able method to recognize processes without much prior knowledge of the parameter dynamics, and without using complementary environmental variables. However, it might be more suitable for recognizing stochastic processes. EMD admits missing data but the gap nature (%; temporal distribution) influences the precision to reveal the large variability time scales. It does not offer information about the relative importance of time scales variability, but it is good method for long-term analysis.

We also demonstrate that the combination of spectral methods opens up new opportunities in the analysis of high-frequency long-term datasets in coastal research. LSP mainly helps SSA in revealing the significant modes and characteristic frequencies. For short-term analysis, SSA complements CWT in the quantification of the contributions of forcings, and CWT complements SSA by offering a more visual time-varying representation. For long-term analysis, EMD gives CWT the opportunity of providing a long-term decomposition, and CWT reveals the time-varying relative importance of time scales in the long-term variability signal from EMD.

The purpose of these comparative analyses was to offer insight into methods of analyzing long-term time-series in coastal systems. The ambition is to be a reference for choosing the most adapted spectral methods as a function of the dataset and requirements. In general, SSA is the most relevant method for the analysis of incomplete high-frequency long-term time series to reveal the importance of forcings affecting a given parameter. Its combination with LSP allows for better identifying processes. These tests are valid for any time series recorded in tidal coastal systems that contain stochastic and deterministic components. For specific questions, combined methods could be more suitable: e.g., EMD or EMD + CWT for signals mainly affected by stochastic processes; CWT or CWT + SSA for short-term analysis. In fact, the use of several methods can provide a more realistic and comprehensive picture of multiscale dynamics.

References

Alvarez-Borrego, J., and S. Alvarez-Borrego. 1982. Temporal and spatial variability of temperature in two coastal lagoons. Calif. Coop. Ocean. Fish. Investig. Rep. **23**: 188–197.

Andersen, T. J., M. Pejrup, and A. A. Nielsen. 2006. Long-term and high-resolution measurements of bed level changes in a temperate, microtidal coastal lagoon. Mar. Geol. **226**: 115–125. doi:10.1016/j.margeo.2005.09.016

Blackman, R. B., and J. W. Tukey. 1958. The measurement of power spectra from the point of view of communication engineering—Part I. Bell Syst. Tech. J. **37**: 485–569. doi: 10.1002/j.1538-7305.1958.tb01530.x

Blain, S., and others. 2004. High frequency monitoring of the coastal marine environment using the MAREL buoy. J. Environ. Monit. **6**: 569–75. doi:10.1039/b314073c

Buschman, F. A., A. J. F. Hoitink, M. Van Der Vegt, and P. Hoekstra. 2009. Subtidal water level variation controlled by river flow and tides. Water Resour. Res. **45**: 1–12. doi: 10.1029/2009WR008167

Camayo, R., and E. J. D. Campos. 2006. Application of wavelet transform in the study of coastal trapped waves off the west coast of South America. Geophys. Res. Lett. **33**, L22601. doi:10.1029/2006GL026395

Castaing, P., and G. P. Allen. 1981. Mechanisms controlling seaward escape of suspended sediment from the Gironde: A macrotidal estuary in France. Mar. Geol. **40**: 101–118. doi:10.1016/0025-3227(81)90045-1

Ciavatta, S., R. Pastres, C. Badetti, G. Ferrari, and M. B. Beck. 2008. Estimation of phytoplanktonic production and system respiration from data collected by a real-time monitoring network in the Lagoon of Venice. Ecol. Modell. **212**: 28–36. doi:10.1016/j.ecolmodel.2007.10.025

Contreras, E., and M. J. Polo. 2012. Measurement frequency and sampling spatial domains required to characterize turbidity and salinity events in the Guadalquivir estuary (Spain). Nat. Hazards Earth Syst. Sci. **12**: 2581–2589. doi:10.5194/nhess-12-2581-2012

Daubechies, I. 1992. Ten lectures on wavelets, p. 357. IEEE Symposium on ComputerBased Medical Systems.

de Jonge, V. N., M. Elliott, and V. S. Brauer. 2006. Marine monitoring: Its shortcomings and mismatch with the EU Water Framework Directive's objectives. Mar. Pollut. Bull. **53**: 5–19. doi:10.1016/j.marpolbul.2005.11.026

Derot, J., F. G. Schmitt, V. Gentilhomme, and S. B. Zongo. 2015. Long-term high frequency phytoplankton dynamics, recorded from a coastal water autonomous measurement system in the eastern English Channel. Cont. Shelf Res. **109**: 210–221. doi:10.1016/j.csr.2015.09.015

Dettinger, M. D., M. Ghil, C. M. Strong, W. Weibel, and P. Yiou. 1995. Software expedites singular-spectrum analysis of noisy time series. Eos (Washington DC) **76**: 12–21. doi:10.1029/EO076i002p00012

Dixon, W., and B. Chiswell. 1996. Review of aquatic monitoring program design. Water Res. **30**: 1935–1948. doi:10.1016/0043-1354(96)00087-5

Dur, G., F. G. Schmitt, and S. Souissi. 2007. Analysis of high frequency temperature time series in the Seine estuary from the Marel autonomous monitoring buoy. Hydrobiologia **588**: 59–68. doi:10.1007/s10750-007-0652-3

Emery, W. J., and R. E. Thomson. 2001. Chapter 3—Statistical methods and error handling, p. 193–304. *In* Data analysis methods in physical oceanography, Emery and Thomson [eds.], Elsevier Science.

Etcheber, H., and others. 2011. Monitoring water quality in estuarine environments: Lessons from the MAGEST monitoring programme in the Gironde fluvial-estuarine system. Hydrol. Earth Syst. Sci. **15**: 831–840. doi:10.5194/hess-15-831-2011

Ezer, T., L. P. Atkinson, W. B. Corlett, and J. L. Blanco. 2013. Gulf Stream's induced sea level rise and variability along the U.S. mid-Atlantic coast. J. Geophys. Res. Ocean. **118**: 685–697. doi:10.1002/jgrc.20091

Farge, M. 1992. Wavelet transforms and their applications to turbulence. Annu. Rev. Fluid Mech. **24**: 395. doi:10.1146/annurev.fl.24.010192.002143

Flandrin, P., and P. Gonçalvès. 2004. Empirical mode decompositions as data-driven wavelet-like expansions. Int. J. Wavelets Multiresolut. Inf. Process. **02**: 477–496. doi:10.1142/S0219691304000561

Flandrin, P., G. Rilling, and P. Goncalves. 2004. Empirical mode decomposition as a filter bank. IEEE Signal Process. Lett. **11**: 112–114. doi:10.1109/LSP.2003.821662

French, J. R., H. Burningham, and T. Benson. 2008. Tidal and meteorological forcing of suspended sediment flux in a muddy mesotidal estuary. Estuaries Coast. **31**: 843–859. doi:10.1007/s12237-008-9072-5

Friedrichs, C. T., and D. G. Aubrey. 1988. Non-linear tidal distortion in shallow well-mixed estuaries: A synthesis. Estuar. Coast. Shelf Sci. **27**: 521–545. doi:10.1016/0272-7714(88)90082-0

Fulcher, B. D., M. A. Little, and N. S. Jones. 2013. Highly comparative time-series analysis: The empirical structure of time series and their methods. J. R. Soc. Interface **10**: 20130048. doi:10.1098/rsif.2013.0048

Gardiner, C. W. 1985. Handbook of stochastic methods for physics, chemistry, and the natural sciences, 2nd ed. Springer-Verlag.

Ghil, M., M. R. Allen, M. D. Dettinger, K. Ide, D. Kondrashov, M. E. Mann, A. W. Robertson, A. Saunders, Y. Tian, F. Varadi, and P. Yiou. 2002. Advanced spectral methods for climatic time series. Rev. Geophys. **40**: 1003. doi:10.1029/2000RG000092

Goberville, E., G. Beaugrand, B. Sautour, and P. Tréguer. 2010. Climate-driven changes in coastal marine systems of western Europe. Mar. Ecol. Prog. Ser. **408**: 129–147. doi:10.3354/meps08564

Grinsted, A., J. C. Moore, and S. Jevrejeva. 2004. Application of the cross wavelet transform and wavelet coherence to geophysical time series. Nonlinear Process. Geophys. **11**: 561–566. doi:10.5194/npg-11-561-2004

Guézennec, L., R. Lafite, J. P. Dupont, R. Meyer, and D. Boust. 1999. Hydrodynamics of suspended particulate matter in the tidal freshwater zone of a macrotidal estuary (The Seine Estuary, France). Estuaries **22**: 717–727. doi:10.2307/1353058

Guo, L., M. Van-der-Wegen, D. A. Jay, P. Matte, Z. B. Wang, D. Roelvink, and Q. He. 2015. River-tide dynamics: Exploration of nonstationary and nonlinear tidal behavior in the Yangtze River estuary. J. Geophys. Res. Ocean. **120**: 3499–3521. doi:10.1002/2014JC010491

Harang, R., G. Bonnet, and L. R. Petzold. 2012. WAVOS: A MATLAB toolkit for wavelet analysis and visualization of oscillatory systems. BMC Res. Notes **5**: 163. doi:10.1186/1756-0500-5-163

Hodges, B. A., and D. L. Rudnick. 2006. Horizontal variability in chlorophyll fluorescence and potential temperature. Deep-Sea Res. Part I Oceanogr. Res. Pap. **53**: 1460–1482. doi:10.1016/j.dsr.2006.06.006

Hoitink, A. J. F. 2004. Tidally-induced clouds of suspended sediment connected to shallow-water coral reefs. Mar. Geol. **208**: 13–31. doi:10.1016/j.margeo.2004.04.021

Huang, N. E., and others. 1998. The empirical mode decomposition and the Hilbert spectrum for nonlinear and non-stationary time series analysis. Proc. R. Soc. A Math. Phys. Eng. Sci. **454**: 903–995. doi:10.1098/rspa.1998.0193

Huang, N. E., Z. Shen, and S. R. Long. 1999. A new view of nonlinear water waves: The Hilbert Spectrum. Annu. Rev. Fluid Mech. **31**: 417–457. doi:10.1146/annurev.fluid.31.1.417

Huang, N. E., H. H. Shih, Z. Shen, S. R. Long, and K. L. Fan. 2000. The ages of large amplitude coastal seiches on the Caribbean Coast of Puerto Rico. J. Phys. Oceanogr. **30**: 2001–2012. doi:10.1175/1520-0485(2000)030<2001:TAO-LAC>2.0.CO;2

Huang, Y. X., F. G. Schmitt, Z. M. Lu, and Y. L. Liu. 2008. An amplitude-frequency study of turbulent scaling intermittency using Empirical Mode Decomposition and Hilbert Spectral Analysis. EPL, Eur. Phys. Soc. **84**: 40010. doi:10.1209/0295-5075/84/40010

Huang, Y., F. G. Schmitt, Z. Lu, and Y. Liu. 2009. Analysis of daily river flow fluctuations using empirical mode decomposition and arbitrary order Hilbert spectral analysis. J. Hydrol. **373**: 103–111. doi:10.1016/j.jhydrol.2009.04.015

Huang, Y., and F. G. Schmitt. 2014. Time dependent intrinsic correlation analysis of temperature and dissolved oxygen time series using empirical mode decomposition. J. Mar. Syst. **130**: 90–100. doi:10.1016/j.jmarsys.2013.06.007

Jalón-Rojas, I., S. Schmidt, and A. Sottolichio. 2015. Turbidity in the fluvial Gironde Estuary (southwest France) based on 10-year continuous monitoring: Sensitivity to hydrological conditions. Hydrol. Earth Syst. Sci. **19**: 2805–2819. doi:10.5194/hess-19-2805-2015, 2015

Jalón-Rojas, I., S. Schmidt, and A. Sottolichio. 2016. Tracking the turbidity maximum zone in the Loire estuary (France) based on a long-term, high-resolution and high-frequency monitoring network. Cont. Shelf Res. **117**: 1–11 doi:10.1016/j.csr.2016.01.017

Jay, D. A., and E. P. Flinchem. 1995. Wavelet transform analyses of non-stationary tidal currents, p. 100–105. Proceedings of the IEEE Fifth Working Conference on Current Measurement.

Kastens, M. 2014. Statistical estuary data analysis in models and measurements—some methods and their limitations. Die Küste **81**: 185–201.

Kbaier, D., I. Puillat, and P. Lazure. In press. Propriétés statistiques de la température, salinité et turbidité mesurées par la station MAREL Carnot dans les eaux côtières de Boulogne-sur-Mer (France). *In* F. G. Schmitt and A. Lefevre [eds.], Mesures haute résolution dans l'environnement marin côtier. Presses du CNRS.

Keiner, L. E., and X.-H. Y. Yan. 1997. Empirical orthogonal function analysis of sea surface temperature patterns in Delaware Bay. IEEE Trans. Geosci. Remote Sens. **35**: 1299–1306. doi:10.1109/36.628796

Kennish, M. J. 2002. Environmental threats and environmental future of estuaries. Environ. Conserv. **29**: 78–107. doi:10.1017/S0376892902000061

Kondrashov, D., and M. Ghil. 2006. Spatio-temporal filling of missing points in geophysical data sets. Nonlinear Process. Geophys. **13**: 151–159.

Kondrashov, D., Y. Shprits and M. Ghil. 2010. Gap filling of solar wind data by singular spectrum analysis. Geophys. Res. Lett. **37**: L15101.

Knowles, N. 2002. Natural and management influences on freshwater inflows and salinity in the San Francisco Estuary at monthly to interannual scales. Water Resour. Res. **38**: 25–1–25–11. doi:10.1029/2001WR000360

Lomb, N. R. 1976. Least-squares frequency analysis of unequally spaced data. Astrophys. Space Sci. **39**: 447–462. doi:10.1007/BF00648343

Luettich, R. A., S. D. Carr, J. V. Reynolds-Fleming, C. W. Fulcher, and J. E. McNinch. 2002. Semi-diurnal seiching in a shallow, micro-tidal lagoonal estuary. Cont. Shelf Res. **22**: 1669–1681. doi:10.1016/S0278-4343(02)00031-6

Machu, E., B. Ferret, and V. Garçon. 1999. Phytoplankton pigment distribution from SeaWiFS data in the subtropical convergence zone south of Africa: A wavelet analysis. Geophys. Res. Lett. **26**: 1469–1472. doi:10.1029/1999GL900256

Matabos, M., A. O. V. Bui, S. Mihály, J. Aguzzi, S. K. Juniper, and R. S. Ajayamohan. 2014. High-frequency study of epibenthic megafaunal community dynamics in Barkley Canyon: A multi-disciplinary approach using the NEPTUNE Canada network. J. Mar. Syst. **130**: 56–68. doi:10.1016/j.jmarsys.2013.05.002

Meyers, S. D., B. G. Kelly, and J. J. O'Brien. 1993. An introduction to wavelet analysis in oceanography and meteorology: With application to the dispersion of Yanai waves. Mon. Weather Rev. **121**: 2858–2866. doi:10.1175/1520-0493(1993)121<2858:AITWAI>2.0.CO;2

Moore, T. S., D. B. Nuzzio, D. M. Di Toro, and G. W. Luther. 2009. Oxygen dynamics in a well mixed estuary, the lower Delaware Bay, USA. Mar. Chem. **117**: 11–20. doi:10.1016/j.marchem.2009.08.003

Nezlin, N. P., K. Kamer, J. Hyde, and E. D. Stein. 2009. Dissolved oxygen dynamics in a eutrophic estuary, Upper Newport Bay, California. Estuar. Coast. Shelf Sci. **82**: 139–151. doi:10.1016/j.ecss.2009.01.004

Pairaud, I., and others. 2013. The MesuRho multi-parameter moored observatory for monitoring of river inputs and extreme events at the Rhone River mouth. 40th CIESM (Mediterranean Science Commission) Congress – Marseille.

Percival, D., and H. Mofjeld. 1997. Analysis of subtidal coastal sea level fluctuations using wavelets. J. Am. Stat. Assoc. **92**: 868–889. doi:10.1080/01621459.1997.10474042

Perillo, G. M. E., and M. C. Piccolo. 2011. Global variability in estuaries and coastal settings, p. 7–36. *In* Treatise on estuarine and coastal science, V. 1: Classification of estuarine and nearshore coastal ecosystems.

Pierson, W. J., and W. Marks. 1952. The power spectrum analysis of ocean-wave records. Trans. Am. Geophys. Union **33**: 834–844. doi:10.1029/TR033i006p00834

Platt, T. 1978. Spectral analysis of spatial structure in phytoplankton populations, p. 73–84. In J. H. Steele [ed.], Spatial pattern in plankton communities. Springer US.

Press, W. H., S. Teukolsky, W. T. Vetterling, and B. P. Flannery. 1992. Numerical recipes in Fortran 77: The art of scientific computing, Cambridge University Press.

Puillat, I., M. Prevosto, H. Mercier, and S. Thomas. 2014. Time series analysis of marine data: A key knowledge at the crossroads of marine sciences. J. Mar. Syst. **130**: 1–3. doi:10.1016/j.jmarsys.2013.11.010

Rabalais, N. N., W. J. Wiseman, and R. E. Turner. 1994. Comparison of continuous records of near-bottom dissolved oxygen from the hypoxia zone along the Louisiana coast. Estuaries **17**: 850–861. doi:10.2307/1352753

Rafelski, L. E., B. Paplawsky, and R. F. Keeling. 2015. Continuous measurements of dissolved O_2 and oxygen isotopes in the Southern California coastal ocean. Mar. Chem. **174**: 94–102. doi:10.1016/j.marchem.2015.05.011

Reynolds-Fleming, J. V., and R. A. Luettich. 2004. Wind-driven lateral variability in a partially mixed estuary. Estuar. Coast. Shelf Sci. **60**: 395–407. doi:10.1016/j.ecss.2004.02.003

Rigby, P., C. R. Steinberg, D. K. Williams, G. Brinkman, H. Tonin, and D. Hughes. 2014. Real-time marine observing systems: Challenges, benefits and opportunities in Australian coastal waters. Aust. J. Civ. Eng. **12**: 83–99. doi:10.7158/C14-015.2014.12.1

Rilling, G., P. Flandrin, and P. Gonçalves. 2003. On empirical mode decomposition and its algorithms. In Proceedings of IEEE-EURASIP Workshop on Nonlinear Signal and Image Processing NSIP-03, Grado (Italy), June 2003.

Różyński, G., M. Larson, and Z. Pruszak. 2001. Forced and self-organized shoreline response for a beach in the southern Baltic Sea determined through singular spectrum analysis. Coast. Eng. **43**: 41–58. doi:10.1016/S0378-3839(01)00005-9

Ruf, T. 1999. The Lomb-Scargle periodogram in biological rhythm research: Analysis of incomplete and unequally spaced time-series. Biol. Rhythm Res. **30**: 178–201. doi:10.1076/brhm.30.2.178.1422

Ruju, A., J. L. Lara, and I. J. Losada. 2014. Numerical analysis of run-up oscillations under dissipative conditions. Coast. Eng. **86**: 45–56. doi:10.1016/j.coastaleng.2014.01.010

Sassi, M. G., and A. J. F. Hoitink. 2013. River flow controls on tides and tide-mean water level profiles in a tidal freshwater river. J. Geophys. Res. C Ocean. **118**: 4139–4151. doi:10.1002/jgrc.20297

Savenije, H. H. G., M. Toffolon, J. Haas, and E. J. M. Veling. 2008. Analytical description of tidal dynamics in convergent estuaries. J. Geophys. Res. Ocean. **113**: 1–18. doi:10.1029/2007JC004408

Scargle, J. D. 1982. Studies in astronomical time-series analysis .2. Statistical aspects of spectral-analysis of unevenly spaced data. Astrophys. J. **263**: 835–853. doi:10.1086/160554

Scavia, D., and others. 2002. Climate change impacts on U.S. Coastal and Marine Ecosystems. Estuaries **25**: 149–164. doi:10.1007/BF02691304

Schmidt, S., H. Etcheber, A. Sottolichio, and P. Castaing. In press. Le réseau MAGEST: bilan de 10 ans de suivi haute-fréquence de la qualité des eaux de l'estuaire de la Gironde. *In* F. G. Schmitt and A. Lefevre [eds.], Mesures haute résolution dans l'environnement marin côtier. Presses du CNRS.

Schmitt, F. G., Y. Huang, Z. Lu, and S. Zongo-Brizard. 2007. Analysis of nonlinear biophysical time series in aquatic environments : Scaling properties and empirical mode decomposition, p. 261–280. *In* A. A. Tsonis and J. B. Elsner [eds.], Nonlinear dynamics in geosciences, Springer New York.

Schmitt, F. G., G. Dur, S. Souissi, and S. Brizard-Zongo. 2008. Statistical properties of turbidity, oxygen and pH fluctuations in the Seine river estuary (France). Phys. A Stat. Mech. Appl. **387**: 6613–6623. doi:10.1016/j.physa.2008.08.026

Schoellhamer, D. H. 1996. Factors affecting suspended-solids concentrations in South San Francisco Bay, California. J. Geophys. Res. **101**: 87–95. doi:10.1029/96JC00747

Schoellhamer, D. H. 2001. Singular spectrum analysis for time series with missing data. Geophys. Res. Lett. **28**: 3187–3190. doi:10.1029/2000GL012698

Schoellhamer, D. H. 2002. Variability of suspended-sediment concentration at tidal to annual time scales in San Francisco Bay, USA. Cont. Shelf Res. **22**: 1857–1866. doi:10.1016/S0278-4343(02)00042-0

Sénéchal, N., P. Bonneton, and H. Dupuis. 2002. Field experiment on secondary wave generation on a barred beach and the consequent evolution of energy dissipation on the beach face. Coast. Eng. **46**: 233–247. doi:10.1016/S0378-3839(02)00095-9

Setz, T. 2011. Wavelet analysis on stochastic time series—a visual introduction with an examination of long term financial time series. ETH Zurich.

Sikora, W., and B. Kjerfve. 1985. Factors influencing the salinity regime of Lake Pontchartrain, Lousiana, a shallow coastal lagoon: Analysis of a long-term data set. Estuaries **8**: 170–180. doi:10.2307/1351866

Torrence, C., and G. P. Compo. 1998. A practical guide to wavelet analysis. Bull. Am. Meteorol. Soc. **79**: 61–78. doi:10.1175/1520-0477(1998)079<0061:APGTWA>2.0.CO;2

Uncles, R. J. 2002. Estuarine physical processes research: Some recent studies and progress. Estuar. Coast. Shelf Sci. **55**: 829–856. doi:10.1006/ecss.2002.1032

Van Dongen, H. P. A., E. Olofsen, J. Van Hartevelt, and E. W. Kruyt. 1997. Periodogram analysis of unequally spaced data: The Lomb method. Department of Physiology, Department of Physiology, Leiden University, Leiden.

Vasseur, D. A., and U. Gaedke. 2007. Spectral analysis unmasks synchronous and compensatory dynamics in

plankton communities. Ecology **88**: 2058–2071. doi: 10.1890/06-1899.1

Vautard, R., P. Yiou, and M. Ghil. 1992. Singular-spectrum analysis: A toolkit for short, noisy chaotic signals. Phys. D **58**: 95–126. doi:10.1016/0167-2789(92)90103-T

Welch, P. 1969. A fixed-point fast Fourier transform error analysis. IEEE Trans. Audio Electroacoust. **17**: 151–157. doi:10.1109/TAU.1969.1162035

Zhang, F., R. Su, J. He, M. Cai, W. Luo, and X. Wang. 2010a. Study on fluorometric discrimination of phytoplankton based on time-series vectors of wavelet transform. Spectrochim. Acta. A. Mol. Biomol. Spectrosc. **75**: 578–584. doi: 10.1016/j.saa.2009.11.020

Zhang, Q., C.-Y. Xu, and Y. Chen. 2010b. Wavelet-based characterization of water level behaviors in the Pearl River estuary, China. Stoch. Environ. Res. Risk Assess. **24**: 81–92. doi:10.1007/s00477-008-0302-y

Zongo, S. B., and F. G. Schmitt. 2011. Scaling properties of pH fluctuations in coastal waters of the English channel: pH as a turbulent active scalars. Nonlinear Process. Geophys. **18**: 829–839. doi:10.5194/npg-18-829-2011

Acknowledgments

I. Jalón-Rojas thanks the Agence de l'Eau Adour-Garonne (AEAG) and the Aquitaine Region for the financial support of her Ph.D. grant. Authors gratefully acknowledge the MAGEST network for turbidity time series. We are also very grateful to Dr. David Schoellhamer for its pertinent review and concrete contributions that helped improve the manuscript.

Submitted 23 November 2015
Revised 12 February 2016
Accepted 17 February 2016

Associate editor: Clare Reimers